

Chondroitin and Dermatan Sulfate Bioinks for 3D Bioprinting and Cartilage Regeneration

Markel Lafuente-Merchan, Sandra Ruiz-Alonso, Alaitz Zabala, Patricia Gálvez-Martín, Juan Antonio Marchal, Blanca Vázquez-Lasa, Idoia Gallego, Laura Saenz-del-Burgo,* and Jose Luis Pedraz*

Cartilage is a connective tissue which has a limited capacity for healing and repairing. In this context, osteoarthritis (OA) disease may be developed with high prevalence in which the use of scaffolds may be a promising treatment. In addition, three-dimensional (3D) bioprinting has become an emerging additive manufacturing technology because of its rapid prototyping capacity and the possibility of creating complex structures. This study is focused on the development of nanocellulose-alginate (NC-Alg) based bioinks for 3D bioprinting for cartilage regeneration to which it is added chondroitin sulfate (CS) and dermatan sulfate (DS). First, rheological properties are evaluated. Then, sterilization effect, biocompatibility, and printability on developed NC-Alg-CS and NC-Alg-DS inks are evaluated. Subsequently, printed scaffolds are characterized. Finally, NC-Alg-CS and NC-Alg-DS inks are loaded with murine D1-MSCs-EPO and cell viability and functionality, as well as the chondrogenic differentiation ability are assessed. Results show that the addition of both CS and DS to the NC-Alg ink improves its characteristics in terms of rheology and cell viability and functionality. Moreover, differentiation to cartilage is promoted on NC-Alg-CS and NC-Alg-DS scaffolds. Therefore, the utilization of MSCs containing NC-Alg-CS and NC-Alg-DS scaffolds may become a feasible tissue engineering approach for cartilage regeneration.

1. Introduction

Osteoarthritis (OA) is the common form of arthritis and it has become the third incapacitating disease after diabetes and dementia.^[1] OA is characterized by structural changes at joint level due to cartilage degradation. Moreover, the increase of extracellular matrix (ECM)-degrading enzymes and inflammatory cytokines^[2] accelerate tissue degradation which result in joints pain, deformity, instability, and reduction of motion and function.^[1,2]

Cartilage is a connective tissue of diarthrodial joints.^[3] It is composed of low metabolic activity cells, chondrocytes, which are surrounded of a highly structured ECM.^[2] ECM is predominately based on water, collagens and glycosaminoglycans (GAGs), and together with chondrocytes, its principal function is to give support to articulations. Cartilage provides a smooth, lubricated surface to articulations and facilitates the transmission of loads with a low

M. Lafuente-Merchan, S. Ruiz-Alonso, I. Gallego, L. Saenz-del-Burgo, J. L. Pedraz
NanoBioCel Group
Laboratory of Pharmaceutics
School of Pharmacy
University of the Basque Country (UPV/EHU)
Vitoria-Gasteiz Spain
E-mail: laura.saenzdelburgo@ehu.es; joseluis.pedraz@ehu.es

M. Lafuente-Merchan, S. Ruiz-Alonso, B. Vázquez-Lasa, I. Gallego, L. Saenz-del-Burgo, J. L. Pedraz
Biomedical Research Networking Center in Bioengineering
Biomaterials and Nanomedicine (CIBER-BBN), Health Institute Carlos III
Monforte de Lemos 3-5, Madrid 28029, Spain


M. Lafuente-Merchan, S. Ruiz-Alonso, I. Gallego, L. Saenz-del-Burgo, J. L. Pedraz
Bioaraba Health Research Institute
Jose Atxotegi, s/n, Vitoria-Gasteiz 01009, Spain

A. Zabala
Mechanical and Industrial Manufacturing Department
Mondragon Unibertsitatea
Loramendi 4, Mondragón 20500, Spain

P. Gálvez-Martín
R&D Animal and Human Health
Bioibérica S.A.U.
Barcelona E-08029, Spain

J. A. Marchal
Biopathology and Regenerative Medicine Institute (IBIMER)
Centre for Biomedical Research
University of Granada
Granada 18100, Spain

J. A. Marchal
Instituto de Investigación Biosanitaria de Granada (ibs.GRANADA)
Andalusian Health Service (SAS)
University of Granada
Granada Spain

 The ORCID identification number(s) for the author(s) of this article can be found under <https://doi.org/10.1002/mabi.202100435>

© 2022 The Authors. Macromolecular Bioscience published by Wiley-VCH GmbH. This is an open access article under the terms of the Creative Commons Attribution-NonCommercial License, which permits use, distribution and reproduction in any medium, provided the original work is properly cited and is not used for commercial purposes.

DOI: 10.1002/mabi.202100435

frictional coefficient.^[3] However, as it is devoid of blood vessels, lymphatic system and nerves, its capacity for healing and repairing is limited.^[2-4] In addition, injuries in this tissue degenerate progressively to very grave diseases such as OA.^[4] Despite the fact that OA has a rising prevalence,^[1] the current pharmacological and surgical treatments are ineffective.^[1,2,5] For this reason, recent therapeutic advances such as gene therapy,^[6] cell therapy,^[7] and tissue engineering^[8] have become promising treatments.^[2]

Tissue engineering is attracting increasing interest, since it allows combining different technologies. It is based on the use of scaffolds, which act not only as supportive cell structures but also as structures that are designed to imitate as closely as possible native tissues.^[2,9,10] Three-dimensional (3D) bioprinting has become an emerging additive manufacturing technology in tissue engineering because of its rapid prototyping capacities and creating complex formulations.^[4,11] It is based on the deposition of biomaterials, either embedded with cells or depositing them later on, in micrometer scale to form structures comparable to biological tissues.^[10,12] However, the deposited biomaterial, termed as bioink when it contains a biological component or as ink when it is cell-free composite, requires specific characteristics in order to imitate the physiological structure of tissues and support living cells.^[12,13]

Chondroitin sulfate (CS) has high potential in bioinks for cartilage regeneration since it is a GAG found in cartilage ECM. It is composed of repeating D-glucuronic acid-*N*-acetylgalactosamine sulfated (disaccharide unit)^[14] and it has numerous biological properties. CS promotes cell differentiation,^[15] the attainment of pluripotency, provides mechanical protection and cell-ECM interactive capability equipping the cell with mechanoresponsive properties.^[16] In addition, it has also anti-inflammatory activity^[14,17] and regulates the metabolism of cartilage tissue.^[14] Apart from its biological activity, physical properties such as water^[16] and nutrient absorption,^[17] cytocompatibility and mechanical strength have been reported.^[16] Thus, CS may help to restore cartilage function and has become a treatment for OA disease.^[15,17]

Similarly to CS, dermatan sulfate (DS) is one of the GAGs in articular cartilage and it is a major component of connective tissue matrix, cell surface and basement membranes.^[18] The chemical composition of DS is the same as that of CS, but it differs in some of the glucuronate residues that undergo epimerization to form iduronate.^[18,19] It has been shown that DS, as other GAGs, could manipulate mesenchymal stromal cells (MSC) behavior regarding adhesion and proliferation.^[20] Moreover, DS plays an impor-

tant role in modulating chondrogenesis and may promote MSC differentiation^[20] and maturation.^[18,21]

Despite the fact that GAGs offer advantages as scaffold components, since they intrinsically have greater stability and lower immunogenicity compared to most ECM proteins,^[20] the addition of other components is often required in order to improve the bioink structural stability.^[22] Alginate (Alg) is a widely used polysaccharide in tissue regenerative fields because of its high water content, biocompatibility and non-toxic properties.^[23-25] Moreover, it offers fast gelling capacity when is mixed with divalent cations, such as calcium, which enables the manufacture of manipulable scaffolds after bioprinting.^[24] In addition, to maintain the structure of the bioprinted scaffolds and improve bioprinting properties, more viscous polymers such as nanofibrillated cellulose (NC) may be added.^[23,26] NC is characterized by high water content, adequate biocompatibility and exceptional physical and chemical properties.^[27] Interestingly, the NC imitates the bulk collagen matrix of the cartilage^[23] so the use of NC-Alg based bioinks in cartilage regeneration has been recently reported in literature.^[23,26]

This study is focused on the development of NC-Alg based bioinks for 3D bioprinting for cartilage regeneration. For this purpose, CS and DS were separately added to NC-Alg inks in order to develop NC-Alg-CS and NC-Alg-DS inks. First, both inks were characterized in terms of rheology, cytotoxicity and printability. Then, scaffolds were printed and their external and inner structure, as well as swelling and degradation kinetics was evaluated. Finally, previously sterilized NC-Alg-CS and NC-Alg-DS inks were loaded with murine D1 MSCs engineered to secrete erythropoietin (D1-MSCs-EPO)^[28] and cell viability, functionality and differentiation to cartilage were assessed.

2. Results and Discussion

One of the main objectives in the field of 3D bioprinting is to develop inks with proper rheological behavior, printability and biocompatibility. Hydrogels based on natural polymers have taken advantage of their high water content and excellent compatibility with cells as well as with native tissues to be selected as ink components among other materials. Thus, we have developed in a previous study,^[29] NC-Alg based bioinks with good results in terms of printability and viability of embedded cells. In the present study, we want to go one step further and demonstrate the ability of these bioinks to form cartilage tissue. Therefore, CS and DS were added, which are naturally found in ECM cartilage and provide different properties such as water^[16] and nutrient absorption,^[17] the enhancement of mechanical properties,^[16] and the promotion of cell proliferation, differentiation and maturation.^[15,20] Then, its effects on inks and scaffolds were evaluated, as well as its benefits on cell viability and cartilage differentiation.

2.1. Ink Fabrication and Rheological Characterization

Different concentrations of CS and DS (1%, 3%, 5%, and 10%) were respectively added to the NC-Alg ink and their rheological behavior was evaluated. In steady flow measurement (**Figure 1**), both, the addition of CS and DS, resulted in a slightly increase on

J. A. Marchal
Department of Human Anatomy and Embryology
Faculty of Medicine
University of Granada
Granada 18016, Spain

J. A. Marchal
BioFab i3D Lab – Biofabrication and 3D (Bio)printing Singular Laboratory
University of Granada
Granada 18100, Spain

B. Vázquez-Lasa
Institute of Polymer Science and Technology
ICTP-CSIC
Juan de la Cierva 3, Madrid 28006, Spain

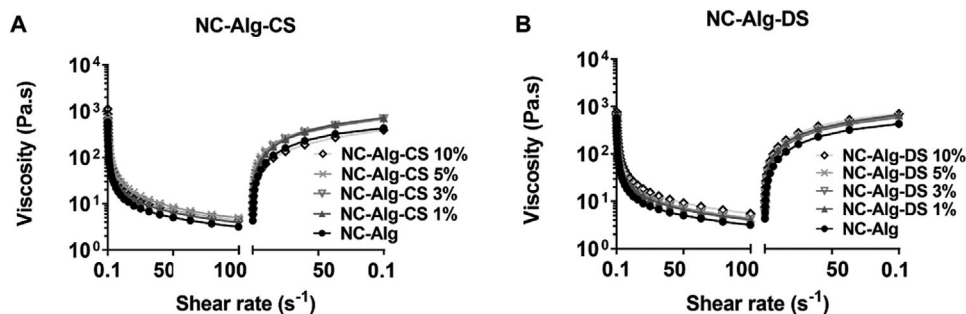


Figure 1. Rheological steady flow measurement of A) NC-Alg-CS inks and B) NC-Alg-DS inks at different concentrations.

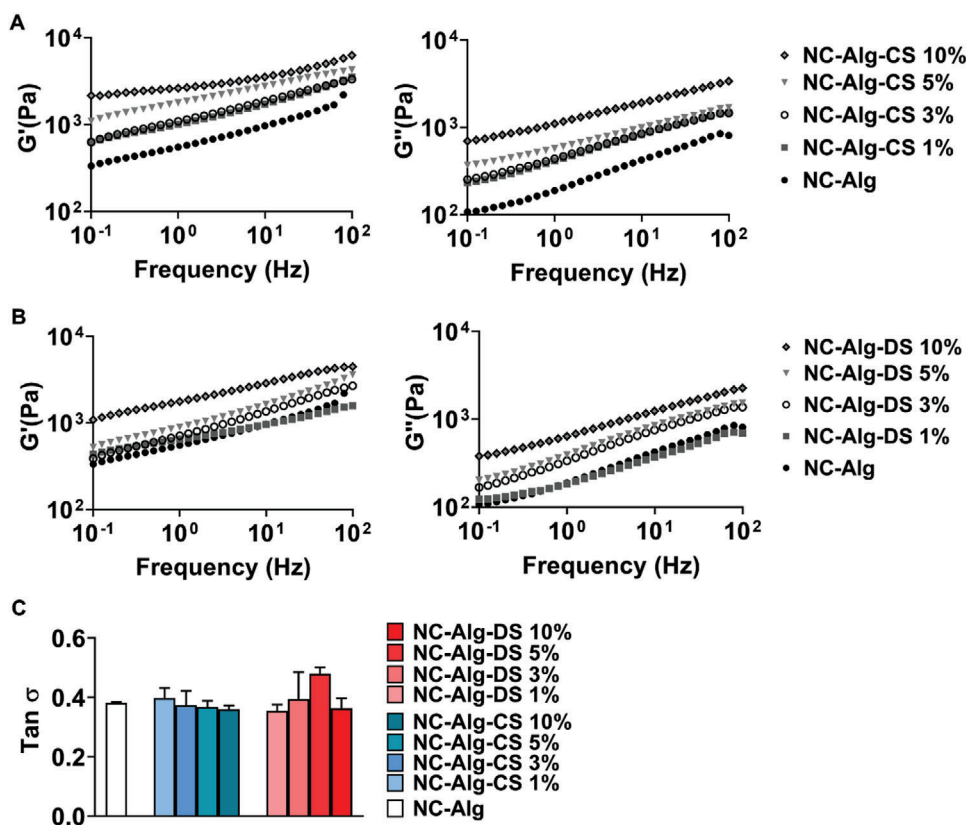


Figure 2. Rheological frequency sweep measurements. Viscoelasticity modules G' and G'' of A) NC-Alg-CS inks and B) NC-Alg-DS inks at different concentrations. C) $\tan \delta$ values of all developed inks. Values represent mean \pm SD.

viscosity values of NC-Alg ink. Moreover, the viscosity increase was proportional to the CS and DS concentrations, being the more viscous inks, the ones composed of NC-Alg-CS 10% and NC-Alg-DS 10%. The relationship between polymer concentration and viscosity explains the increase of viscosity when higher proportion of CS or DS was added.^[13]

Interestingly, all formulations showed shear thinning behavior as viscosity values decrease under shear rate, with a recovery on viscosity when the shear rate was returned to initial values. Shear thinning behavior is essential to print through extrusion as viscosity of the ink must decrease to pass through the printer needle. Besides, when the ink is deposited on the printer bed, the viscosity must return to initial so as to maintain scaffold shape.

Despite the fact that all formulations met these properties, inks containing CS showed higher viscosity values in comparison with NC-Alg-DS inks. However, the NC-Alg-CS 10% ink in Figure 1A, showed a lower viscosity recovery, which would indicate less capacity to maintain the shape fidelity of the scaffolds after printing compared to its equivalent NC-Alg-DS 10% in which this effect was not seen (Figure 1B).

On the other hand, frequency sweep rheological measurement was performed in order to evaluate viscoelastic properties of the inks with different concentrations of CS and DS. The results in Figure 2 show the elastic modulus (G') and viscous modulus (G'') of the inks at different frequencies. The addition of both, CS (Figure 2A) and DS (Figure 2B), resulted in an increase in viscoelastic

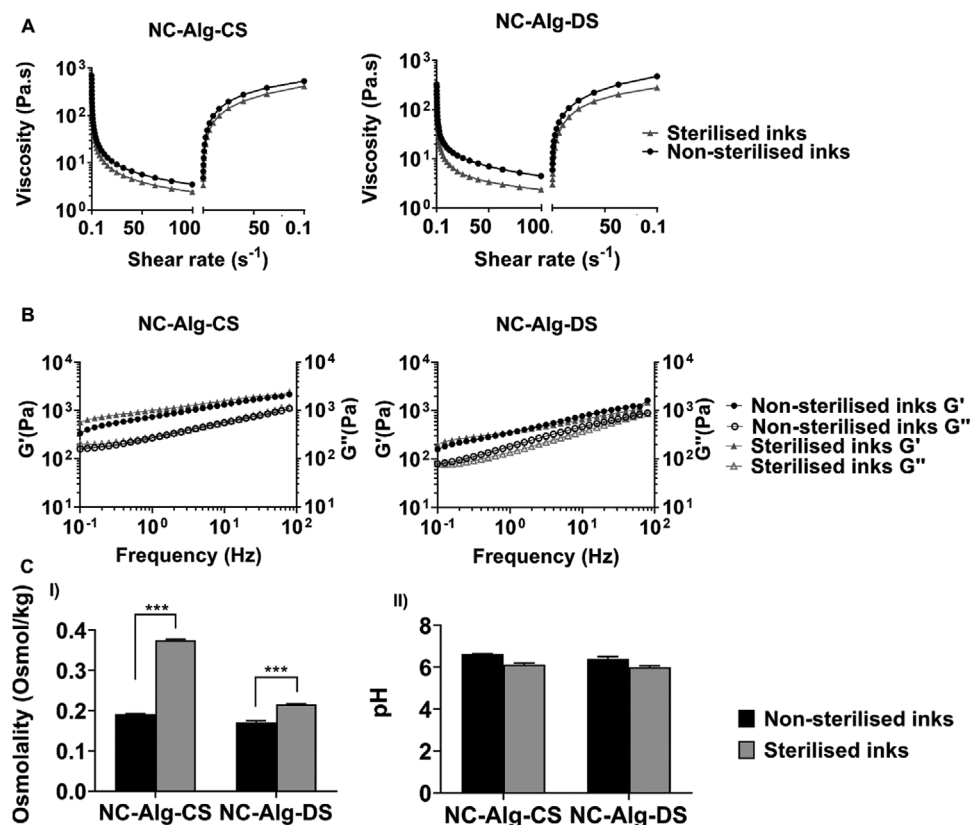


Figure 3. Evaluation of the sterilisation procedure on NC-Alg-CS and NC-Alg-DS inks properties. A) Rheological steady flow measurement. B) Frequency sweep rheological measurement. C) Physicochemical study I) Osmolality and II) pH values represent mean \pm SD. *** $p < 0.001$.

values in comparison with the NC-Alg ink, being this increase proportional to the CS and DS concentrations. Although both, CS and DS, increased the values of G' and G'' , differences were observed between them. In fact, the inks containing CS showed higher viscoelasticity values (Figure 2A). It has been reported that GAGs have naturally good viscoelastic properties due to their chemical composition, since a high viscosity allows a good lubrication of the joint and a good rigidity provides protection against mechanical damage.^[30,31]

In addition, the relation between G''/G' was evaluated by the value of $\tan \delta$ in Figure 2C. According to the literature, values of $\tan \delta$ close to 1 indicate that the inks extrude uniformly and require low extrusion pressures, nevertheless, exhibit poor shape fidelity. On the other hand, inks with $\tan \delta$ closer to 0 are robust, but require higher printing pressures and a uniform extrusion is difficult.^[32] Among fabricated inks, no significant differences were observed. Results showed $\tan \delta$ values between 0 and 1, which indicated that all NC-Alg-CS and NC-Alg-DS inks were feasible to be printed by extrusion. In fact, all the values were between 0.35–0.47 which has been demonstrated to be optimal for balancing smooth extrusion, shape fidelity, and cell viability in alginate-gelatin bioinks.^[33]

According to the rheological studies, the addition of different concentrations of CS and DS improves proportionally viscosity and viscoelastic properties of the base NC-Alg ink. Despite the fact that all the formulations were feasible to be printed by extrusion, the concentration of 10% of CS and DS seemed to be the

best option to create well defined scaffolds. However, bioinks with values of G' below 5000 Pa require less extrusion pressures when are printed, and, therefore, are better for cell viability.^[32] The ink containing 10% CS reached values of G' of 6000 Pa. Thus, it was discarded. In contrast the formulation containing 10% of DS did not exceed this value, but it was also discarded in order to observe the differences after adding CS and DS with an equivalent concentration. As a consequence, the following formulations of NC-Alg-CS 5% and NC-Alg-DS 5% were elected to perform the following experimental studies.

2.2. Rheological and Physicochemical Evaluation after Sterilization

Before incorporating cells into the NC-Alg-DS and NC-Alg-CS inks, complete sterility must be ensured. Therefore, inks were sterilized by short cycle autoclave, which was already demonstrated to be the less harmful method for NC-Alg inks.^[29] Sterility tests indicated that NC-Alg based inks were free of containing microorganisms since no turbidity was detected after sterilization (data not shown). Then, it was verified if the process had changed fundamental properties for 3D bioprinting such as rheology and physicochemical properties.

As it can be seen in Figure 3A, a slight decrease in viscosity was observed. However, the two inks maintained the shear thinning behavior and the ability to recover the viscosity after finishing the

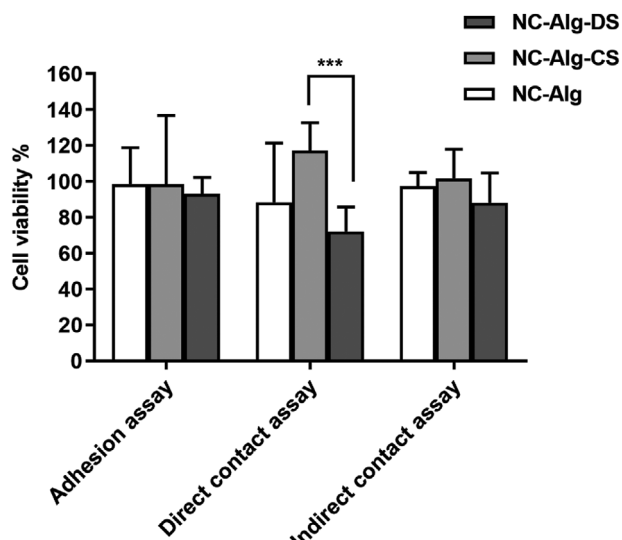


Figure 4. Cytotoxicity evaluation of NC-Alg-CS and NC-Alg-DS inks in adhesion, direct contact and indirect contact assays. Values represent mean \pm SD. *** $p < 0.001$.

pressure, which suggests that no problems when being printed can be expected. In addition, the viscoelastic properties were not modified (Figure 3B). In fact, the G' and G'' values were very similar between non-sterile and sterile inks for both, NC-Alg-CS and NC-Alg-DS inks.

On the other hand, the pH and osmolality of the inks were evaluated after sterilization (Figure 3C). No significant variations were observed after sterilization for all formulations in pH measurements in comparison with non-sterile inks (Figure 3CII). Conversely, osmolality was affected by sterilization. All the inks showed (Figure 3CI) an increase in osmolality values after autoclaving ($p < 0.001$). A degradation has been reported, in terms of molecular weight loss, in biopolymers after heating, which would cause the release of osmotically active solutes to the media,^[34] and, therefore, the increase of osmolality values in the inks. Nevertheless, these changes in osmolality were not detrimental to cells that were subsequently embedded, since high viability values were observed in biological studies.

According to rheological and physicochemical properties, inks maintained the properties to be feasible to be printed through extrusion bioprinter.

2.3. Cytotoxicity Evaluation

For 3D bioprinting, a successful ink must meet not only with good rheological properties, but also with good biocompatibility. To evaluate biocompatibility of NC-Alg-CS and NC-Alg-DS inks, the adhesion, direct contact and indirect contact cytotoxicity tests were performed in concordance with the ISO 10993-5-2009.^[35]

As it is shown in **Figure 4**, in the adhesion assay, the addition of CS and DS to the NC-Alg ink demonstrated high cell viability which was similar to NC-Alg ink. Similarly, indirect contact assay showed high cell viability of L929 fibroblasts and no significant differences among the inks (NC-Alg-CS ink $101.85 \pm 16.10\%$, NC-Alg-DS ink $92.31 \pm 16.50\%$ and NC-Alg ink $97.35 \pm 7.65\%$).

On the other hand, the percentage of live cells after direct contact test was high in all the cases, although statistically significant differences were observed between NC-Alg-CS and NC-Alg-DS inks, being cell viability higher on NC-Alg-CS inks ($p < 0.001$). The contribution of GAGs such as chondroitin and dermatan in cellular behavior has been previously reported in many studies.^[20,36] In fact, in the consulted literature it has not been seen that dermatan was more toxic than chondroitin. Therefore, this difference was due to the ability of the cells to adhere to NC-Alg-DS ink, which implied that fewer cells remained in the well plate and cell viability was lower than in the other inks. Anyway, in accordance with ISO standards, a reduction on cell viability by more than 30% is considered as a potentially cytotoxic effect. Consequently, the evaluated inks did not present cytotoxicity.

2.4. 3D Printing and Printability Evaluation

Once the inks were characterized, printing studies were carried out. At the time of printing 15 mm grid-like scaffolds, differences were observed between the parameters to be applied in the bioprinter. The NC-Alg ink required printing pressures of 25 kPa, while the inks containing CS and DS needed pressures close to 30 kPa. These differences were due to the increase in viscosity and viscoelasticity that CS and DS produced in the inks. In addition, these rheological improvements resulted in differences in the obtained scaffolds, being CS (**Figure 5C**) and DS (**Figure 5D**) printed scaffolds the ones that resembled the best the computer assisted design (**Figure 5A**). In fact, diameter measurements of the printed scaffolds resulted in higher shape fidelity on NC-Alg-CS scaffolds (NC-Alg-CS scaffolds 15.34 ± 0.05 mm, NC-Alg-DS scaffolds 15.86 ± 0.32 mm and NC-Alg scaffolds 16.26 ± 0.24 mm vs the 15 mm of the computerized design). Moreover, closer images of the scaffolds demonstrated that in the scaffolds containing CS the grid structure was squarer, which implies more similarity to the design. In contrast, in the scaffold with DS a more oval grid structures were observed, being the NC-Alg scaffolds the one that differed the most from the original design. Alginate based inks have been found to have difficulties in obtaining printed scaffolds with high resolution.^[37] For this reason, the addition of viscous materials such as gelatin or nanocellulose has proven to be effective in obtaining scaffolds with good printability that maintain shape fidelity when compared to computerized design.^[38,39] In a recent study it has been seen that inks composed of nanocellulose and 2.5–5% alginate have good results in terms of printability.^[38] In this study, 2% alginate was used, so a lower resolution in NC-Alg scaffolds could be expected. The addition of both CS and DS improved the rheological properties and, therefore, the resolution and shape fidelity of the printed scaffolds were enhanced.

2.5. Scaffold Characterization

2.5.1. Surface and Architectural Study

NC-Alg, NC-Alg-CS, and NC-Alg-DS scaffolds were characterized using optical profilometry in order to obtain an in-depth evaluation of scaffolds surface and architecture. As **Figure 6A** shows,

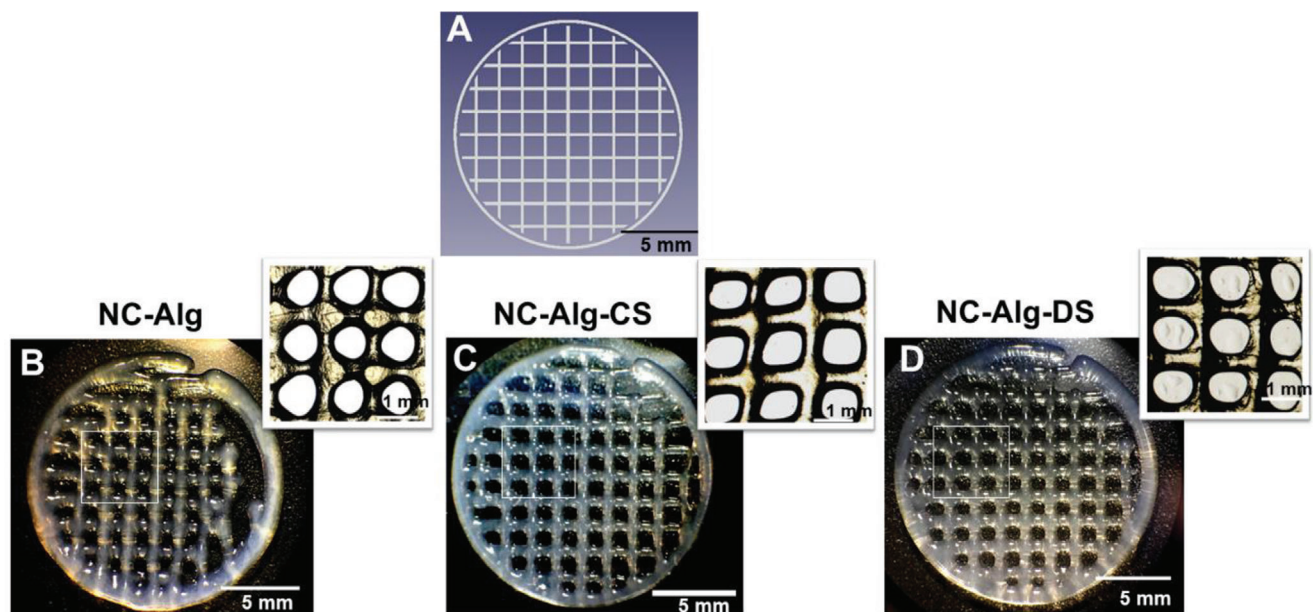


Figure 5. Printability study. A) Computer assisted design of the scaffolds. B) Macroscopic images of printed scaffolds being NC-Alg, C) NC-Alg-CS, and D) NC-Alg-DS. Scale bar 5 and 1 mm.

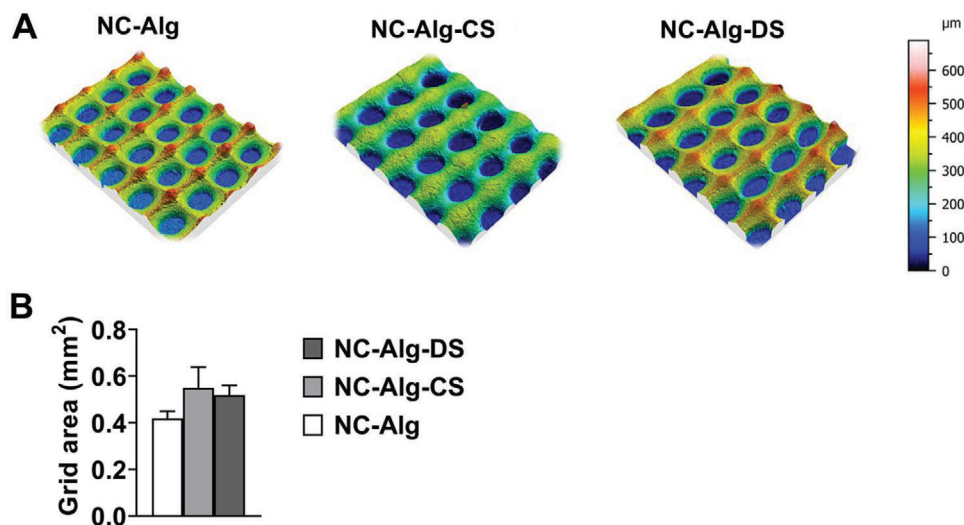


Figure 6. Surface and architectural characterization on NC-Alg, NC-Alg-CS and NC-Alg-DS scaffolds. A) Images of topology measurements and binarized areas of the printed scaffolds. B) Grid area measurements from binarized data analysis. Values represent mean ± SD.

differences were observed among scaffolds. The CS scaffolds showed less height compared to the DS and NC-Alg scaffolds, suggesting a greater resemblance to the computerized scaffold that was designed with a height of 200 μm for each layer and, therefore, 400 μm at the intersections. In fact, when the area of the grid was analyzed (Figure 6B), the scaffolds containing CS were the ones that most closely resembled the theoretical grid area value of the design of 0.6 mm² (NC-Alg-CS scaffolds grid area 0.55 ± 0.09 mm², NC-Alg-DS grid area 0.52 ± 0.04 mm² and NC-Alg scaffolds grid are 0.42 ± 0.03 mm²).

In addition, the layer thickness and height of scaffolds were analyzed in Figure 7. The printing process was carried out with

a 0.2 mm needle diameter according to the thickness of each layer pre-established by the design. As Figure 7A shows, the layer thickness was slightly higher in all scaffolds than in the original design. Furthermore, differences between the thickness in the X direction and in the Y direction were observed, being thicker in the Y direction. Although no statistically significant differences were shown among scaffolds, the ones containing DS and NC-Alg demonstrated higher thickness in the X direction compared to scaffolds with CS. On the other hand, the height of the scaffolds layers was slightly higher in the Y direction than in the X direction (Figure 7B). When a comparison is made, scaffolds containing DS were statistically higher in the X direction ($p < 0.001$)

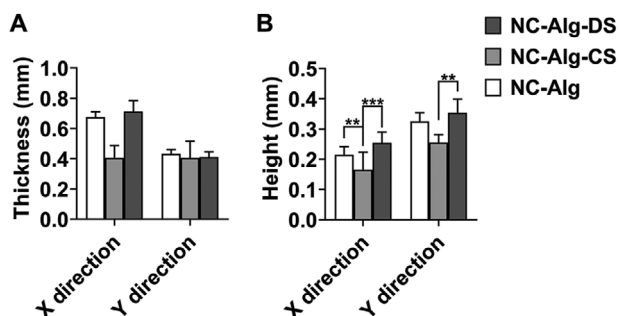


Figure 7. Surface and architectural characterization on NC-Alg, NC-Alg-CS, and NC-Alg-DS scaffolds. Evaluation of the strut architecture of the printed scaffolds in terms of A) thickness and B) height. Values represent mean \pm SD. *** $p < 0.001$, ** $p < 0.01$.

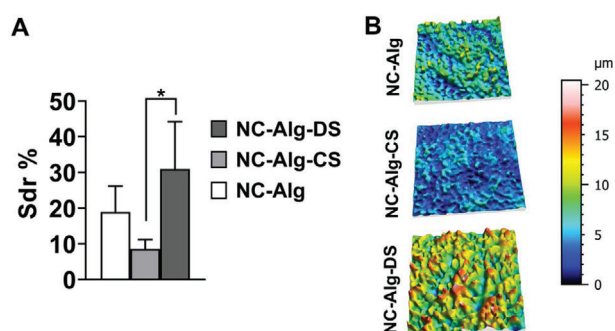


Figure 8. Surface and architectural structure characterization on scaffolds. A) 3D topographical parameters describing hybrid (Sdr) characteristics of the NC-Alg, NC-Alg-CS, and NC-Alg-DS scaffolds. Values represent mean \pm SD. * $p < 0.05$. B) Representative axonometric projections of the topographical measurements of scaffolds.

and in the Y direction ($p < 0.01$) in comparison with NC-Alg-CS scaffolds. Moreover, NC-Alg scaffolds height in X direction was also higher than scaffolds containing CS ($p < 0.01$). The good rheological properties that exhibited CS inks support these results, which show a height and thickness in both X and Y directions, more similar to those established by the computer design and the printing needle. On the contrary, a lower viscoelasticity in NC-Alg-DS and NC-Alg inks caused them to flow more in the printing process, obtaining thicker structures.

These results reinforce the conclusion drawn from the printability study, in which the addition of CS to the ink improved the resemblance of printed scaffolds to the original design in comparison with inks containing DS. As a consequence, and taking into account the rheological studies, it can be concluded that in terms of printability and the formation of scaffolds, the addition of CS to the NC-Alg ink is better than the addition of DS.

Finally, the roughness of the scaffolds was evaluated (see Figure 8). Scaffolds containing DS showed an increase in roughness that was visualized in the Sdr parameter, this rise being significant in comparison with scaffolds containing CS ($p < 0.05$). In addition, the Sdr % was lower in CS scaffolds than in NC-Alg scaffolds. These differences were also observed in topographical images in Figure 8B, in which a higher rough surface was observed in NC-Alg-DS scaffolds whereas a smoother surface was observed in scaffolds containing CS. It has been reported that roughness

is related to the success of the implant, thus, in clinical trials, it has been seen that the roughest implants have higher survival rates than the smoothest ones, when implanted in tissues such as bone.^[40] Furthermore, a rough topography has shown to improve MSCs adhesion.^[41,42] Taking into account the importance of the roughness on cell behavior, a greater cellular adhesion may be expected in the NC-Alg-DS scaffolds. However, it would be necessary to deepen with in vivo studies to evaluate these differences among scaffolds after implantation.

2.5.2. Scanning Electron Microscopy (SEM)

NC-Alg-CS and NC-Alg-DS printed scaffolds were evaluated by SEM in order to evaluate the external and internal structures. As Figure 9 shows, scaffolds containing CS showed similar external structure to the DS scaffolds. In addition, a higher quantity of fibers was observed in both, CS and DS scaffolds, in comparison with NC-Alg scaffolds. Then, crosscut was made to observe the internal structure of all the scaffolds so as to ascertain their porosity. A porous scaffold implies an exchange of fluids and nutrients that would be necessary for embedded cells viability.^[43] All scaffolds showed a porous internal structure and, therefore, the assurance of the cells to be maintained alive inside them.

2.5.3. Swelling and Degradation

The swelling behavior is an important property of printed scaffolds and tissue engineering as it is related to the diffusion of nutrients and signaling molecules.^[44] Figure 10A shows the swelling behavior of NC-Alg-CS and NC-Alg-DS scaffolds. NC-Alg scaffolds were used as controls. Results demonstrated good swelling properties for both scaffolds, which was to be expected due to the high water absorption capacity of the biopolymers that were used for printing the scaffolds.^[45] Interestingly, scaffolds containing CS and DS showed a statistically significant lower water uptake ability in comparison with NC-Alg scaffolds in the majority of studied times. Swelling degree is usually related to the crosslinking density, consequently, inks with high dense inner structures show a decrease in swelling degree.^[46] The addition of CS and DS to the base ink formed by NC-Alg showed an increase in viscosity and viscoelastic properties indicating a denser structure, which would explain the lower swelling behavior.

On the other hand, Figure 10B shows the degradation study of NC-Alg-CS and NC-Alg-DS scaffolds. Degradation studies are of great importance for regenerative medicine because it may affect the medical application. An ideal degradation performs with the regeneration or replacement of native tissue while the scaffold is being degraded.^[47] Both scaffolds, showed the same degradation behavior, being the first 24 h when the reduction of the scaffold area was more important ($p < 0.05$). Furthermore, there were no differences in comparison with the scaffold without CS and DS. In fact, after 10 days of study the area reduction of NC-Alg-CS scaffolds were 73 ± 3.40 , NC-Alg-DS scaffolds 79.85 ± 0.05 and NC-Alg scaffolds 78.62 ± 7.21 . Thus, the NC-Alg based scaffolds showed a controlled degradation behavior over the time, which would imply good medical applicability. Cartilage is a complex and specific tissue in which is difficult to estimate the optimal

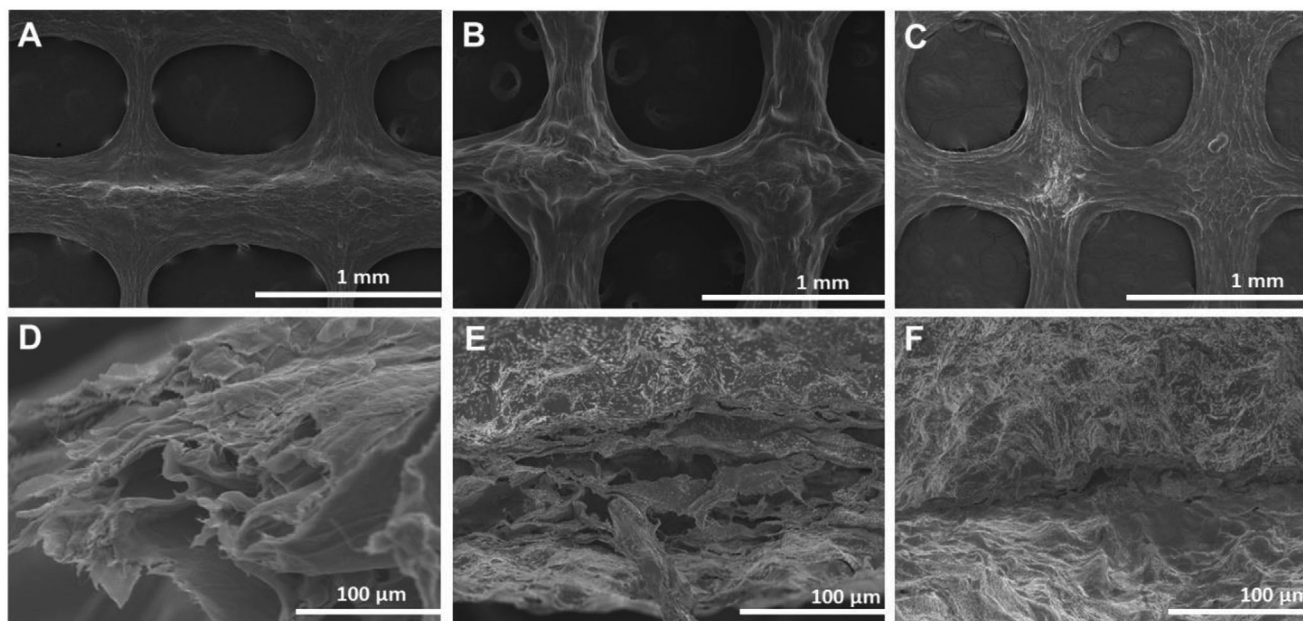


Figure 9. Representative of A–D) scanning electron images of NC-Alg, B–E) NC-Alg-CS scaffolds, and C–F) NC-Alg-DS scaffolds. Scale bar in (A) and (B): 1 mm and in (C) and (D): 100 μm .

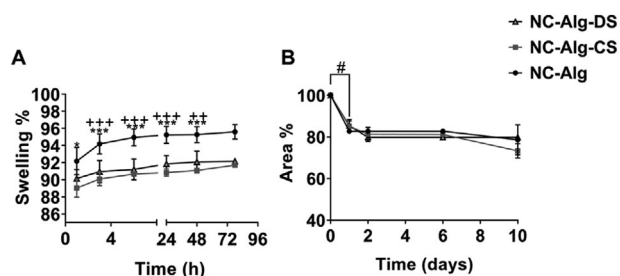


Figure 10. NC-Alg-CS and NC-Alg-DS printed scaffolds A) swelling determination and B) degradation rate. NC-Alg scaffolds were used as controls. Values represent mean \pm SD. *** $p < 0.001$; * $p < 0.05$ comparison between NC-Alg-CS and NC-Alg scaffolds. +++ $p < 0.001$; ++ $p < 0.01$ comparison between NC-Alg-DS and NC-Alg scaffolds. # $p < 0.05$, comparison between days in the same scaffolds.

biodegradation time of tissue engineered scaffolds. Therefore, the time required for tissue regeneration depends on the cartilage defect identification, function and the location.^[48] In addition, the degradation rate could be modified by making chemical modifications to the alginate. Thus, phosphorylated alginate has been applied to fabricate hydrogels that were more resistant to degradation.^[49] Alternatively, degradation kinetics have been also controlled by varying the molecular weight of the alginate.^[50] However, in vivo studies need to be carried out to study in depth the degradation processes.

2.5.4. Mechanical Properties

Mechanical properties of scaffolds were analyzed because cartilage is a tissue that is subjected to great forces of tension and compression. Thus, compression Young's modulus was obtained

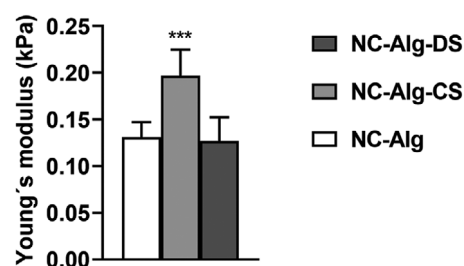


Figure 11. Young's modulus analysis of printed NC-Alg-CS, NC-Alg-DS, and NC-Alg scaffolds. Values represent mean \pm SD. *** $p < 0.001$.

as an intrinsic material property that describes the material's stiffness or resistance to elastic deformation under load.

Results showed in **Figure 11** a significant increase in the Young's modulus in the scaffolds containing CS ($p < 0.001$). On the other hand, NC-Alg-DS scaffolds showed similar values to the control scaffold composed of NC-Alg. It has been previously described in the literature that CS is responsible for the mechanical resistance of tissues such as cartilage through the electrostatic repulsions of its sulfate groups.^[16,51,52] Furthermore, contrary to CS, it has been suggested that DS has no effect on mechanical properties, which would explain the results obtained in this study.^[53] Despite the increase in terms of mechanical properties after the addition of CS, all the printed scaffolds did not approach the values of native cartilage (0.2–2 MPa).^[54] The mechanical properties of cartilage derive from its complex composition and well-organized internal structure.^[53] The scaffolds used in this study were immature as they did not contain chondrocytes to secrete matrix components that enhance mechanical properties such as collagen. In addition, compression modulus is strongly subjected to the solid content. In this study, printed scaffolds

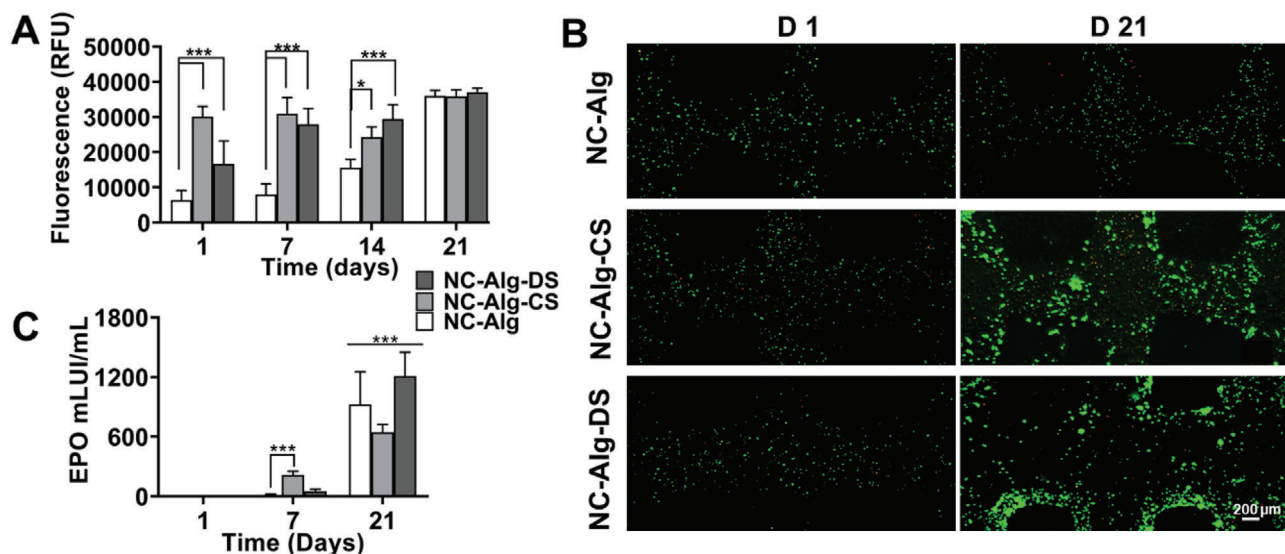


Figure 12. Cell viability and functionality studies inside NC-Alg-CS, NC-Alg-DS, and NC-Alg scaffolds. A) Metabolic activity assay. B) Representative fluorescence micrographs of live/dead stained scaffolds, showing live (green) and dead (red) cells at day 1 and 21 after bioprinting. Scale bar 200 μ m. C) EPO release quantification. Values represent mean \pm SD. *** $p < 0.001$; * $p < 0.05$.

showed around 90–95% of water content, whereas cartilage is composed of 70–80% fluid.^[55] For this reason, hydrogel-based materials are usually employed to perform in local injuries in conjunction with cartilage tissue instead of substitutes of the total tissue.

2.6. Biological Analysis

2.6.1. Cell Viability, Metabolism, and Functionality Evaluation

For tissue engineering applications, the survival of the cells within the ink is essential. In this study, D1-MSCs-EPO was introduced into the bioink and their viability and functionality were analyzed after 21 days of bioprinting. MSCs have the potential to differentiate into chondrocytes among other cell types, thus, their use in the field of tissue engineering to regenerate cartilage is quite wide.^[56,57] Furthermore, cells genetically modified to release EPO were used due to the fact that its functionality inside the ink can be easily measured. A cell density of 5×10^6 cells mL^{-1} was elected since high cell densities as well as the pneumatic pressure applied during bioprinting may be stressful for embedded cells and in vitro quantification at low cell densities may result problematic. This was verified in a previous study in which cell densities of 1×10^6 cells mL^{-1} showed low cell viability and metabolic activity inside NC-Alg scaffolds.^[29] In this study, we tested if the addition of CS and DS to the NC-Alg scaffolds can enhance cell viability and metabolism, as well as, functionality. As it is shown in **Figure 12A**, metabolic activity of D1-MSCs-EPO increased over the time after bioprinting, which suggests cell proliferation inside the scaffolds. Interestingly, the addition of CS and DS improved cells metabolism at 1, 7, and 14 days after bioprinting in comparison with the control scaffold composed only of NC-Alg. Furthermore, the improvement in cell metabolism was significantly greater ($p < 0.001$) in the NC-Alg-DS scaffolds

during the first three studied times after bioprinting. Similarly, cells inside NC-Alg-CS scaffolds showed higher metabolic activity at days 1 and 7 after bioprinting ($p < 0.001$) and at day 14 ($p < 0.05$) in comparison with control scaffolds. At day 21, all the scaffolds showed similar cell metabolic activity. The increase in cell metabolism during the first days after bioprinting may be due to the fact that bioinks with higher viscoelastic properties protect encapsulated cells from the stress caused by the bioprinting process itself.^[58] As shown in the rheological results, the addition of CS and DS increased these properties of the ink and, consequently, the cell viability after bioprinting is expected to be higher than in the NC-Alg scaffolds.

D1-MSCs-EPO viability was analyzed by the Live/Dead staining at day 1 and 21 after bioprinting. The results in **Figure 12B** show that the cells inside all the scaffolds were homogeneously distributed. When a comparison was made, no visual differences were observed at day 1 after bioprinting among all the scaffolds in which live cells were predominant (in green). On the contrary, at day 21 after bioprinting, higher fluorescent intensity was observed in the live cells of the scaffolds containing CS and DS, which may suggest higher cell viability in these scaffolds than in the NC-Alg scaffolds. In fact, after analyzing the images using Image J software to show the percentage between cells alive (in green) and dead (in red), it was seen that NC-Alg-DS scaffolds showed $88.14 \pm 2.62\%$ cell viability, NC-Alg-CS scaffolds showed $80.11 \pm 1.85\%$ cell viability and NC-Alg scaffolds showed $77.77 \pm 6.80\%$ cell viability. Furthermore, cell aggregates were observed in the CS and DS scaffolds, which has been demonstrated to favor the differentiation of MSCs into chondrocytes.^[59] Surprisingly, this visual appreciation does not agree with the studies of cell metabolism, since it would be expected that the higher the cell viability, the higher the metabolism. Possibly, more quantitative techniques might give us more accurate cell viability data. However, what is certain is the involvement of CS and DS in cellular biological processes, which has been reported in another

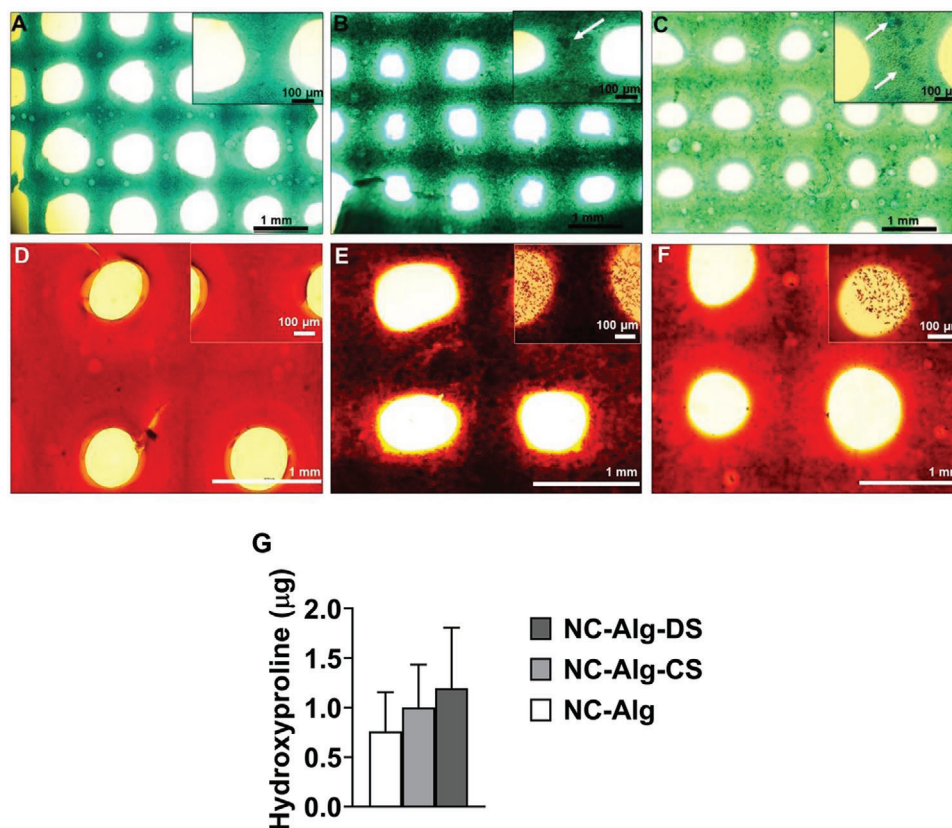


Figure 13. Chondrogenic differentiation evaluation of bioprinted scaffolds. Alcian blue staining of A) NC-Alg scaffolds, B) NC-Alg-CS scaffolds, and C) NC-Alg-DS scaffolds. D) Safranin-O staining of NC-Alg scaffolds, E) NC-Alg-CS scaffolds, and F) NC-Alg-DS scaffolds. G) Hydroxyproline quantification of bioprinted scaffolds. Values represent mean \pm SD. Scale bar 1 mm and 100 μ m.

studies.^[15,60] In fact, cell viability as well as cell metabolic activity have been reported to increase in scaffolds containing both CS and DS.^[16,21]

Finally, in order to evaluate the functionality of the cells embedded in the NC-Alg-CS and NC-Alg-DS scaffolds, the release of EPO hormone was evaluated after bioprinting. As Figure 12C shows, there was no EPO release on day 1 after bioprinting in any of the scaffolds, which could be explained by the stress suffered by the cells during the bioprinting process. However, at day 7, a slight increase in the EPO release was observed in all the scaffolds. Moreover, this increase was more significant ($p < 0.001$) in the scaffolds containing CS compared to the controls, NC-Alg scaffolds. At the end of the assay, the release of the hormone increased significantly compared to day 1 and 7, with the scaffolds containing DS being the ones with the highest EPO release (NC-Alg-DS 1209.34 ± 240.88 mLUI mL⁻¹, NC-Alg-CS 643.98 ± 78.74 mLUI mL⁻¹ and NC-Alg 925.21 ± 327.99 mLUI mL⁻¹). Results suggest that cells maintained their functionality inside all scaffolds after bioprinting. The increase in the production of EPO by the cells may be related to the boost of metabolic activity and viability at day 21. The release of EPO hormone by MSCs has already been described in cells embedded in alginate hydrogels.^[61] Furthermore, it has been possible to obtain a controlled release of EPO in vivo in hyaluronic hydrogels as drug carrier systems.^[62] In this study, the obtained scaffolds show a good release of the hormone

and, therefore, may be used for the release of therapeutic agents.

2.6.2. Differentiation Evaluation to Cartilage

Once it has been studied that the NC-Alg-CS and NC-Alg-DS scaffolds enhance the viability of embedded D1-MSC-EPO, their capacity to differentiate to cartilage was evaluated. In this case, unmodified D1-MSC were used as they have already shown to be able to differentiate into chondrocytes, osteocytes, and adipocytes when they are encapsulated in alginate and hyaluronic hydrogels.^[61]

After 21 days in culture with differentiating medium, the bioprinted NC-Alg-CS and NC-Alg-DS scaffolds were stained with Alcian blue, which stains GAGs, and Safranin-O (red), which detects cartilage. NC-Alg scaffolds were used as controls. As it can be seen in Figure 13, differences were observed among the stained scaffolds. In the scaffolds containing DS (Figure 13C), darker areas were observed with the alcian blue staining, which indicates the production of GAGs by the embedded cells. Moreover, darker areas were also observed in the CS scaffolds (Figure 13B) with this staining. Additionally, NC-Alg-CS and NC-Alg-DS scaffolds stained with safranin-O showed darker areas as well as the cells that had been released from the scaffolds were stained (Figure 13E,F). Conversely, in the scaffolds without CS or

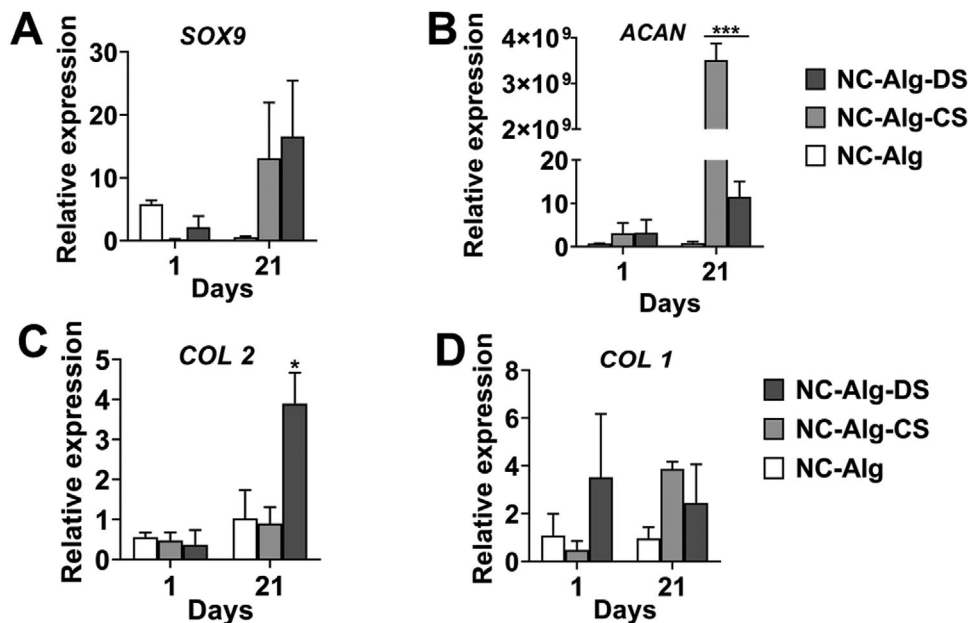


Figure 14. Chondrogenic gene expression of D1-MSCs embedded on NC-Alg, NC-Alg-CS, and NC-Alg-DS bioprinted scaffolds. RT-PCR was carried out after 1 and 21 days of bioprinting. Values represent mean \pm SD. *** $p < 0.001$; * $p < 0.05$.

DS (Figure 13A–D) these dark areas were not appreciated, which indicates a greater degree of differentiation in the scaffolds containing CS and DS.

Then, the hydroxyproline assay was carried out to quantify the production of collagen, which, being one of the components of the cartilage ECM, would indicate the capacity of bioprinted scaffolds to produce a niche similar to the biological one. Results in Figure 13G show that hydroxyproline was detected in all the scaffolds. Nevertheless, no statistically significant differences were observed among them. However, the scaffolds containing DS and CS seem to have higher amounts of hydroxyproline compared to the NC-Alg scaffolds. This may indicate that there is an ECM production similar to native cartilage, which would indicate differentiation of D1-MSCs within the scaffolds to chondrocytes. It was observed in a study using chitosan scaffolds that the joint addition of dermatan and chondroitin increased collagen deposition, however, it was also suggested that the deposition of other components of the ECM such as GAGs is more accentuated.^[63] In another study based on hyaluronic scaffolds, a higher deposition of GAGs was also observed than of collagen accumulation.^[64] In this study, a GAG quantification was not performed, which could have given us a closer approximation of cartilage ECM production than that of collagen accumulation in which no significant differences between scaffolds were observed.

The stainings, together with the quantification of collagen by the hydroxyproline assay, indicate that in the presence of CS and DS, the D1-MSCs have higher ability to differentiate to cartilage. In fact, it has already been reported previously that both, CS and DS, regulate chondrogenesis and promote maturation and differentiation of mesenchymal stem cells.^[20]

Next, in order to obtain a more in-depth evaluation of the differentiation degree to cartilage, RT-PCR studies were carried out. In this study, the expression of chondrogenic marker genes such as aggrecan (ACAN), collagen type 1 and 2 (COL1, COL2), and

SOX9 was analyzed. As it is shown in Figure 14, the relative expression of all the genes was measured after 1 and 21 days of bioprinting. As Figure 14A shows, the NC-Alg-CS and NC-Alg-DS scaffolds obtained an increase in expression of the SOX9 gene at day 21 after bioprinting compared to the NC-Alg scaffolds, which decreased compared to day 1. SOX9 is a chondrogenic transcription factor that regulates chondrocyte differentiation and cartilage ECM production.^[65] Furthermore, greater differences were observed when it comes to the ACAN gene expression (Figure 14B). Scaffolds containing DS increased significantly ($p < 0.001$) the ACAN expression on day 21 compared to day 1 and NC-Alg scaffolds. In addition, interestingly enough, the NC-Alg-CS scaffolds showed a significantly higher amplified ACAN expression ($p < 0.001$) at day 21 in comparison with other kind of scaffolds. The ACAN gene is a chondrogenic differentiation marker as well as the major structural component of the cartilage tissue.^[4] It has been proven that in the presence of CS, the hMSCs seeded onto the scaffolds accelerate chondrogenesis and maintain their chondrogenic phenotype.^[14] Moreover, it has been shown that after the oral administration of CS in OA patients, the production of proteoglycans is increased,^[66,67] which may explain the high expression of this gen in the scaffolds containing CS. In addition, COL2 is also a chondrogenic marker as indicates suitable ECM production necessary for cartilage regeneration.^[14] The highest increase of this gene at day 21 was only observed in the DS scaffolds ($p < 0.05$), while in both the CS and control scaffolds only a slight increase was seen (Figure 14C). In a chondrogenesis differentiation, COL2 increases while COL1 decreases, since COL1 is expressed in undifferentiated chondrocytes or other intermediate cells such as fibroblasts and osteoblasts.^[68]

As Figure 14D shows, in the NC-Alg-DS scaffolds, COL1 decreases slightly on day 21, indicating, together with the increase in COL2 and ACAN, differentiation to cartilage. On the other hand, the expression of COL1 was increased in the CS scaffolds,

which may indicate no chondrogenic differentiation. However, the high expression of ACAN indicates a cartilaginous tissue. Overall, cells embedded in CS and DS scaffolds satisfactorily expressed cartilage phenotype compared to cells inside the NC-Alg scaffolds.

3. Conclusions

The study focuses on whether the addition of CS and DS improves the characteristics of the ink based on NC-Alg as well as the observation of the biological effects on bioprinted scaffolds with these components. The CS showed better results than the DS in terms of rheological properties, which was reflected in the printability study. In addition, scaffolds surface and architectural studies reinforced these results, as the scaffolds with CS had a greater similarity to the computerized design than the DS scaffolds. The characterization in terms of SEM, swelling and degradation resulted in similarities between the contribution of CS and DS on the NC-Alg scaffolds. However, the addition of CS resulted in higher scaffold mechanical properties than DS scaffolds. On the other hand, in the *in vitro* results, a greater improvement was seen when adding DS than CS in the metabolic activity and functionality of embedded D1-MSCs-EPO. Furthermore, both DS and CS induced cells to express genes that indicated differentiation to cartilage, being the DS scaffolds the ones that followed a more typical cartilaginous gene expression profile.

Overall, both, the addition of CS and DS, improved the characteristics of the NC-Alg based bioink. While the CS provided an improvement in printability, the DS showed better biological properties of the embedded cells. Although the combination of the two elements in a single bioink may be the best option, this study showed that the NC-Alg-DS ink would be the preference choice to achieve scaffolds feasible for their application in cartilage tissue engineering.

4. Experimental Section

Materials: Ultra-pure low-viscosity high guluronic acid sodium alginate (UPLVG) was obtained from FMC Biopolymer (Sandvika, Norway). Chondroitin sulfate and dermatan sulfate were acquired from Bioiberica (Barcelona, Spain). Nanofibrillated cellulose was obtained from Sappi Europe (Brussels, Belgium). D-mannitol, calcium chloride, and 3-(4,5-dimethylthiazol-2-yl)-2,5-diphenyltetrazoliumbromid (MTT) *in vitro* toxicology assay were acquired from Sigma-Aldrich (Madrid, Spain). Fetal bovine serum (FBS), fetal calf serum (FCS), and penicillin/streptomycin (P/S) were obtained from Gibco (San Diego, USA). DPBS code BE17-513F was purchased from Lonza (Porriño, Spain). Alamar blue was purchased from Bio-Rad científica (Madrid, Spain). LIVE/DEAD Viability/Cytotoxicity kit was purchased from Life Technologies (Madrid, Spain).

Inks Formulation: Different concentrations of CS and DS were proposed in order to fabricate the inks: 1%, 3%, 5%, and 10% (w/v). To prepare NC-Alg-CS ink, Alg and CS powders were dissolved in a D-mannitol solution to a final 2% (w/v) and 1%, 3%, 5%, and 10% (w/v) concentrations, respectively. Afterward, NC was incorporated at 80% (v/v) proportion of the final solution and everything was mixed until complete homogenization.

The NC-Alg-DS ink was fabricated similarly by dissolving Alg and DS powders in a D-mannitol solution to a final 2% (w/v) and 1%, 3%, 5%, and 10% (w/v) concentrations, respectively. Subsequently, NC was added at 80% (v/v) proportion of the final solution and everything was mixed until complete homogenization.

Inks Characterization: Rheological Study: Rheological properties of all bioinks were measured on the AR100 rheometer from TA Instruments (New Castle, USA). In order to analyze viscosity, steady flow measurements were conducted through a shear rate sweep from 0.1 to 100 s⁻¹. Then, a second sweep from 100 to 0.1 s⁻¹ was set. On the other hand, oscillatory shear measurements were carried out to evaluate the inks viscoelasticity properties (elastic modulus (G') and viscous modulus (G'')), oscillation frequency sweeps were set from 0.1 to 100 Hz and strain was established in 2%. Tan δ values were obtained from the G''/G' relation. Studies were carried out at room temperature using a flat geometry. Three replicates per experiment were conducted.

Sterilization Process and Evaluation of Its Effect on the Inks: Fabricated inks were sterilized using short cycle autoclave that was previously reported to be the less harmful technique.^[29] This procedure was conducted by AJL Ophthalmic (Miñano, Spain) in an industrial autoclave FOA2/B model. The short autoclave started at 15–18 °C temperature and at 0.96 bar pressure. Then, for 22 min the temperature and pressure increased until being established at 123–124 °C and 3.70–3.60 bar, respectively. With these parameters set, the sterilization occurred for 3.04 min. Subsequently, cooling process occurred for 26 min with a decrease in the temperature and pressure to 50–55 °C and 1.60 bar. Finally, after 54 min, the autoclave cycle ended with around 50 °C temperature and 1.05 bar pressure.

Afterward, the sterilization effect on inks properties was evaluated. First, sterility test was conducted for NC-Alg based inks by carrying out a direct inoculation of 1 mL of sample in the microbiological medium to determine for the growth of anaerobic, and aerobic bacteria, fungi, and yeast, in accordance with the European Pharmacopeia.^[69] Then, previously aforementioned rheological studies were carried out. In addition, a cryoscopic osmometer Osmomat 030-D from Gonotec (Berlin, Germany) was used to determine the osmolality. For this study, 50 μL of each ink was evaluated by quantifying the freezing point depression. On the other hand, a pH-meter GLP 21 from Crison (Barcelona, Spain) was used to determine the pH. Each sample was assayed in triplicate.

Cytotoxicity Study: Three different assays were carried out to determine *in vitro* cytotoxicity of the inks in concordance with the ISO 10993-5-2009:^[35] Direct and indirect cytotoxicity and adhesion assays. Mouse L929 fibroblasts were used to perform all the experiments and a cell density of 3.123 × 10⁴ cells cm⁻² was established to seed the cells.

In the direct and indirect cytotoxicity assays cells were seeded and maintained in culture for 24 h. Afterward, they were exposed directly to the NC-Alg, NC-Alg-CS, and NC-Alg-DS circular scaffolds placing them onto the seeded cells in the direct assay, or by adding conditioned media (media that has been in contact with the scaffolds for 24 h) in the indirect cytotoxicity test. After 24 h, cell viability was estimated in both assays using MTT *in vitro* toxicity assay kit following manufacture's recommendations. Cells with no scaffold exposure or cells not exposed to conditioned media were used as controls. On the other hand, in the adhesion assay, cells were seeded directly onto the scaffolds. After 4 h cell viability was quantified using the same MTT procedure. Cells directly seeded onto the plate were used as controls.

In all assays, an Infinite M200 microplate reader from TECAN Trading AG (Männedorf, Switzerland) was used to determine the absorbance at 570 nm with reference wavelength set at 650 nm. Cell viability was calculated using Equation (1):

$$\text{Cell viability (\%)} = \frac{\text{Testing sample OD}_{570}}{\text{Untreated blank OD}_{570}} \times 100 \quad (1)$$

Six independent assays were carried out with three replicates per assay. In concordance with the ISO 10993-5-2009, a cell viability above 70% was contemplated as non-toxic.

3D Printing: An extrusion-based 3D bioprinter Bio X from Cellink (Gothenburg, Sweden) was used to print the inks. Circular grid-like scaffolds of 15 mm diameter and 2 layers were printed using a 27 G conical needle. Printing parameters were established at 4–5 mm s⁻¹ printing speed and 25–30 kPa extrusion pressure for all inks. After printing,

crosslinking process was carried out by submerging the scaffolds in a 100×10^{-3} M calcium solution for 5 min.

Afterward, scaffolds were observed under a Nikon AZ100 microscope from Izasa Scientific (Barcelona, Spain) in order to take macroscopic images.

Scaffolds Characterization: Surface and Architectural Structure Study: An optical profilometer from Sensofar S-NEOX (Barcelona, Spain) through focus variation method was used to characterize the surface topography and architecture of the scaffolds. A metrological software SensoMAP Premium 7.4 from Digital Surf (Besançon, France) was applied to post-process all the measurements. The scaffolds were analyzed in hydrated state after wiping with a dry lint free wipe.

To perform the architectural analysis, a $6484 \times 4880 \mu\text{m}^2$ area measurement was acquired at 3 locations on 3 independently printed samples for each condition using a $10\times$ objective (side sampling: $1.29 \mu\text{m}$, vertical resolution: 25 nm). The thickness and height of the deposited strut were measured and a quantification of the deposited material volume was carried out through the 3D parameter V_m .^[70] Then, measurements were binarized, and in order to analyze the pore morphology, the aspect ratio ($D_{\text{max}}/D_{\text{min}}$) was determined. To evaluate the surface topography, a measurement of $873 \times 656 \mu\text{m}^2$ at 3 independent areas were acquired using a $20\times$ objective (lateral sampling: $0.65 \mu\text{m}$, vertical resolution: 8 nm). 3D topographical parameter belonging hybrid (Sdr) from ISO 25178-2^[71] was determined on cropped areas of $150 \times 150 \mu\text{m}^2$.

Scanning Electron Microscopy (SEM): After critical point drying, an Emitech K550X ion-sputter was used to coat the scaffolds with a thin layer of gold (≈ 15 nm). Afterward, a Hitachi S-3400 Scanning Electron Microscope from Hitachi (Illinois, USA) was used to observe the samples using a 15 kV voltage and around 20 mm of working distance.

Swelling Study: NC-Alg-CS and NC-Alg-DS printed scaffolds of $0.4 \times 15 \text{ mm}^2$ were used in order to analyze the swelling behavior. First, a Telstar cryodos Freeze Dryer (Terrassa, Spain) was used to lyophilize all the scaffolds. Then, they were weighted to determine the dried weight. Finally, to evaluate their swelling capacity, dried scaffolds were submerged in Dulbecco's phosphate-buffered saline (DPBS) with calcium and magnesium at 37°C . At chosen time points, scaffolds were removed from DPBS, water excess was removed using filter paper and scaffolds were reweighed. NC-Alg scaffolds were used as controls. The % of swelling was computed in every time point by using Equation (2):

$$\text{Swelling (\%)} = \frac{W_{\text{wet}} - W_{\text{dried}}}{W_{\text{dried}}} \times 100 \quad (2)$$

where W_{wet} and W_{dried} are wet weight and dried weight, respectively.

Degradation Study: NC-Alg-CS and NC-Alg-DS scaffolds area was calculated to analyze the degradation process. Afterward, scaffolds were placed in DMEM at 37°C and, at selected time points, the area was measured again. Then, samples were returned to the culture medium after conducting the measurements, NC-Alg scaffolds were used as controls. The area loss in % was computed by using Equation (3):

$$\text{Area loss (\%)} = \frac{A_{\text{before}} - A_{\text{after}}}{A_{\text{before}}} \times 100 \quad (3)$$

where A_{before} and A_{after} correspond to the scaffold area before introducing in DMEM and after passing selected time in DMEM.

Mechanical Properties: NC-Alg-CS and NC-Alg-DS scaffolds of 15 mm diameter and 0.4 mm height were analyzed in a TA.XT.plusC Texture Analyser from Aname Instrumentación Científica (Madrid, Spain) to determine mechanical properties. A compression test was performed with a load cell of 5 kg and 20 mm cylinder probe. Test speed was set at 0.5 mm s^{-1} and at maximum of 80% strain. Compression Young's modulus was determined as the slope of stress-strain curve in the linear elastic range. Six replicates per sample were conducted and NC-Alg scaffolds were used as control.

D1-MSCs-EPO Culture Conditions, Bioinks Preparation, and 3D BIO-PRINTING: Murine D1-MSCs purchased from ATCC (Virginia, USA)

were engineered to secrete erythropoietin (D1-MSCs-EPO).^[28] T-flasks with DMEM supplemented with 10% (v/v) FBS and 1% (v/v) P/S were used to perform the cell culture. Cells were sustained at 37°C in a humidified atmosphere containing 5% CO_2 . They were subcultured at 80% confluence and culture medium was regularly replaced.

To carry out 3D bioprinting process, the inks were developed as previously mentioned (see Section 2.2). Then, a 5×10^6 cells mL^{-1} density was incorporated into the inks using a cell mixer device in order to obtain the bioinks. Afterward, they were bioprinted following the aforementioned process (see Section 2.4). Crosslinking procedure was carried out after bioprinting by submerging the scaffolds for 5 min in a 100×10^{-3} M CaCl_2 . Finally, they were deposited in complete medium for their culture. The whole process was conducted under aseptic conditions and at room temperature.

Biological Studies of Bioprinted Scaffolds: Metabolic Activity Determination: The AlamarBlue assay (AB) was used to determine the metabolic activity of embedded D1-MSCs-EPO. The process was performed by placing bioprinted circular grid-like scaffolds of 15 mm diameter in 24 well plates with a solution containing 10% of AB in complete medium. Next, a 4 h of incubation at 37°C was carried out. Finally, an Infinite M200 microplate reader from TECAN Trading AG (Männedorf, Switzerland) was used to read the fluorescence at excitation 560 and 590 nm emission wavelength. Wells containing culture media were used as negative controls. At least twelve samples were conducted for each condition.

Qualitative Cell Viability Determination by Fluorescence Microscopy: The LIVE/DEAD Viability/Cytotoxicity Kit was used to evaluate weekly cell viability. Scaffolds were rinsed in DPBS and placed in the staining solution with 100×10^{-3} M calcein AM. After an incubation of 40 min at room temperature and protected from de light, the calcein solution was removed to add a solution containing 0.8×10^{-6} M ethidium homodimer-1. Then, scaffolds were incubated for 10 min at 37°C . Finally, samples were washed again with DPBS and a Nikon TMS microscope (Virginia, USA) was used to observe them. It was set a wavelength of excitation 495 nm per emission 515 nm (for calcein AM staining) and excitation 495 nm per emission 635 nm (for ethidium homodimer staining). At least three independent tests were conducted for each condition. Afterward, the obtained images were analyzed with the image J software to quantify the percentage of live and dead cells.

EPO Secretion: EPO secretion was determined using Quantikine IVD Human EPO ELISA Kit from R&D Systems (Madrid, Spain). The secretion for 24 h from supernatants at days 1, 7, and 21 after bioprinting was quantified. Cell embedded scaffolds were incubated with 500 μL of DMEM for 24 h at 37°C . Then supernatants were collected. Supernatants without scaffolds were used as controls. Three independent samples for each condition were assayed.

Differentiation: Chondrogenic Differentiation: NC-Alg, NC-Alg-CS, and NC-Alg-DS scaffolds containing 5×10^6 D1-MSCs mL^{-1} were differentiated into chondrocytes. Chondrogenic differentiation medium was composed of DMEN-High glucose from ATCC (Virginia, USA) supplemented with 10% fetal bovine serum, 1% P/S, 10 ng mL^{-1} TGF- β 1, 50×10^{-9} M L-ascorbic acid and 6.25 $\mu\text{g mL}^{-1}$ bovine insulin, all purchased from Merck (Madrid, Spain). Scaffolds were cultured in differentiation medium which was changed every 3 days for 21 days. Complete medium without supplements was used for the culture of controls.

Histological Staining and Collagen Production: After 21 days of culture with differentiation medium, scaffolds were washed with DPBS and fixed with 4% formaldehyde. To evaluate chondrogenic differentiation of embedded D1-MSC scaffolds were stained with Alcian Blue and Safranin-O, both purchased from Merck (Madrid, Spain). Afterward, scaffolds were observed under a Nikon AZ100 microscope from Izasa Scientific (Barcelona, Spain).

The total collagen secreted by chondrocytes in the scaffolds was estimated by hydroxyproline assay kit from Merck (Madrid, Spain). Scaffolds were digested in acid solution after 1 and 21 days of culture and hydroxyproline was quantified following the manufacturer instructions. L-hydroxyproline was used as a standard and scaffolds without differentiation medium were used as negative controls. The absorbance was read at

550 nm on an Infinite M200 microplate reader from TECAN Trading AG (Männedorf, Switzerland). Results were expressed as D21/D1, where D21 (final value) is the amount of hydroxyproline at day 21 and D1 (initial value) at day 1.

Gene Expression by RT-PCR: The chondrogenic effect of NC-Alg-CS and NC-Alg-DS scaffolds was evaluated using a quantitative real-time PCR assay. NC-Alg scaffolds were used as controls. Scaffolds were disaggregated incubating them for 15 min at 37 °C in 1 mg mL⁻¹ alginate lyase and 1.5% (w/v) sodium citrate, both purchased from Merck (Madrid, Spain). Total mRNA was extracted using TRIzol Reagent and was quantified with a SimpliNano nanodrop from GE Healthcare Life Sciences (Madrid, Spain). The conversion of RNA to cDNA was performed using Fast Gene Scriptase II, cDNA Synthesis Kit from Genetics Nippon Europe (Düren, Germany). Real-time PCRs were performed using StepOnePlus Real-Time PCR Systems from Fisher Scientific (Madrid, Spain). Fluorogenic qRT-PCR-based (TaqMan) assay and specific primers for ACAN, COL1, COL2, and SOX9 were used to quantify the target genes. The expression of all genes was normalized to the housekeeping gene glyceraldehyde-3-phosphate dehydrogenase (GAPDH) and to gene expression of untreated samples. Relative expression was calculated with the 2^{-ΔΔCT} method.

Statistical Analysis: IBM SPSS software was applied to conduct the statistical analysis. Data were expressed as mean ± standard deviation and differences were considered significant when *p* < 0.05. Student's *t*-test to identify significant differences between two groups and ANOVA to multiple comparisons were used. Depending on the results of the Levene test of homogeneity of variances, Bonferroni or Tamhane post-hoc test was applied. For non-normally distributed data, Mann–Whitney nonparametric analysis was applied.

Acknowledgements

The authors thank the Basque Government for granted fellowship to S. Ruiz-Alonso (PRE_2020_2_0143). This study was financially supported by the Basque Country Government (IT907-16), the Ministerio de Economía, Industria y Competitividad (FEDER funds, project RTC-2016-5451-1). They also wish to thank the intellectual and technical assistance from the ICTS “NANBIOSIS,” more specifically by the Drug Formulation Unit (U10) of the CIBER in Bioengineering, Biomaterials & Nanomedicine (CIBER-BBN) at the University of Basque Country (UPV/EHU). This research was also supported by Fundación Mutua Madrileña (project FMM-AP17196-2019), Consejería de Economía, Conocimiento, Empresas y Universidad de la Junta de Andalucía (ERDF funds, projects B-CTS-230-UGR18, SOMM17-6109, and P18-FR-2465), and the Instituto de Salud Carlos III, ERDF funds (DTS19/00145 and DTS21/00098). The authors also thank to Spanish Ministry of Science and Innovation (MICINN) (project PID2020-114086RB-I00). The corresponding author information was updated on March 14, 2022.

The copyright line for this article was changed on 27 May 2022 after original online publication.

Conflict of Interest

The authors declare no conflict of interest.

Data Availability Statement

Research data are not shared.

Keywords

3D bioprinting, bioinks, cartilage, chondroitin sulfate, dermatan sulfate, tissue engineering

Received: October 26, 2021
Revised: December 28, 2021
Published online: January 22, 2022

- [1] G. A. Hawker, *Clin. Exp. Rheumatol.* **2019**, *120*, 3.
- [2] L. Roseti, G. Desando, C. Cavallo, M. Petretta, B. Grigolo, *Cell* **2019**, *8*, 1305.
- [3] A. J. Sophia Fox, A. Bedi, S. A. Rodeo, *Sports Health* **2009**, *1*, 461.
- [4] Y. P. Singh, A. Bandyopadhyay, B. B. Mandal, *ACS Appl. Mater. Interfaces* **2019**, *11*, 33684.
- [5] A. Ghouri, P. G. Conaghan, *Clin. Exp. Rheumatol.* **2019**, *37*, S124.
- [6] E. C. Rodriguez-Merchan, L. A. Valentino, *Arch. Bone Jt. Surg.* **2019**, *7*, 79.
- [7] R. Zhang, J. Ma, J. Han, W. Zhang, J. Ma, *Am. J. Transl. Res.* **2019**, *11*, 6275.
- [8] S. Vega, M. Kwon, J. Burdick, *Eur. Cells Mater.* **2017**, *33*, 59.
- [9] W. Zhu, X. Ma, M. Gou, D. Mei, K. Zhang, S. Chen, *Curr. Opin. Biotechnol.* **2016**, *40*, 103.
- [10] S. Derakhshanfar, R. Mbeleck, K. Xu, X. Zhang, W. Zhong, M. Xing, *Bioact. Mater.* **2018**, *3*, 144.
- [11] L. Valot, J. Martinez, A. Mehdi, G. Subra, *Chem. Soc. Rev.* **2019**, *48*, 4049.
- [12] P. S. Gungor-Ozkerim, I. Inci, Y. S. Zhang, A. Khademhosseini, M. R. Dokmeci, *Biomater. Sci.* **2018**, *6*, 915.
- [13] K. Hölzl, S. Lin, L. Tytgat, S. Van Vlierberghe, L. Gu, A. Ovsianikov, *Biofabrication* **2016**, *8*, 032002.
- [14] P. Agrawal, K. Pramanik, V. Vishwanath, A. Biswas, A. Bissoyi, P. K. Patra, *J. Biomed. Mater. Res., Part B* **2018**, *106*, 2576.
- [15] M. Bishnoi, A. Jain, P. Hurkat, S. Jain, *Glycoconjugate J.* **2016**, *33*, 693.
- [16] B. L. Farrugia, M. S. Lord, J. M. Whitelock, J. Melrose, *Biomater. Sci.* **2018**, *6*, 947.
- [17] J. H. Elisseeff, S. Fermanian, D. Wang, B. Sharma, S. Varghese, D. H. Fairbrother, I. Strehin, J. Gorham, B. Cascio, *Nat. Mater.* **2007**, *6*, 385.
- [18] C. B. Foldager, C. Bünger, A. B. Nielsen, M. Ulrich-Vinther, S. Munir, H. Everland, M. Lind, *Int. Orthop.* **2012**, *36*, 1507.
- [19] J. Valcarcel, R. Novoa-Carballal, R. I. Pérez-Martín, R. L. Reis, J. A. Vázquez, *Biotechnol. Adv.* **2017**, *35*, 711.
- [20] B. E. Uygun, S. E. Stojsih, H. W. T. Matthew, *Tissue Eng., Part A* **2009**, *15*, 3499.
- [21] Y.-L. Chen, H.-P. Lee, H.-Y. Chan, L.-Y. Sung, H.-C. Chen, Y.-C. Hu, *Biomaterials* **2007**, *28*, 2294.
- [22] M. I. Neves, M. Araújo, L. Moroni, R. M. P. Da Silva, C. C. Barrias, *Molecules* **2020**, *25*, 978.
- [23] D. Nguyen, D. A. Hägg, A. Forsman, J. Ekholm, P. Nimkingratana, C. Brantsing, T. Kalogeropoulos, S. Zaunz, S. Concaro, M. Britberg, A. Lindahl, P. Gatenholm, A. Enejder, S. Simonsson, *Sci. Rep.* **2017**, *7*, 658.
- [24] E. Axpe, M. Oyen, *Int. J. Mol. Sci.* **2016**, *17*, 1976.
- [25] F. Yu, X. Han, K. Zhang, B. Dai, S. Shen, X. Gao, H. Teng, X. Wang, L. Li, H. Ju, W. Wang, J. Zhang, Q. Jiang, *J. Biomed. Mater. Res., Part A* **2018**, *106*, 2944.
- [26] M. Müller, E. Öztürk, Ø. Arlov, P. Gatenholm, M. Zenobi-Wong, *Ann. Biomed. Eng.* **2017**, *45*, 210.
- [27] A. Sheikhi, J. Hayashi, J. Eichenbaum, M. Gutin, N. Kuntjoro, D. Khorasani, A. Khademhosseini, *J. Controlled Release* **2019**, *294*, 53.
- [28] H. Gurruchaga, J. Ciriza, L. Saenz Del Burgo, J. R. Rodriguez-Madoz, E. Santos, F. Prosper, R. M. Hernández, G. Orive, J. L. Pedraz, *Int. J. Pharm.* **2015**, *485*, 15.
- [29] M. Lafuente-Merchan, S. Ruiz-Alonso, A. Espona-Noguera, P. Galvez-Martin, E. López-Ruiz, J. A. Marchal, M. L. López-Donaire, A. Zabalá, J. Ciriza, L. Saenz-Del-Burgo, J. L. Pedraz, *Mater. Sci. Eng., C* **2021**, *126*, 112160.
- [30] T. J. Lujan, C. J. Underwood, N. T. Jacobs, J. A. Weiss, *J. Appl. Physiol.* **2009**, *106*, 423.
- [31] A. Silipo, Z. Zhang, F. J. Cañada, A. Molinaro, R. J. Linhardt, J. Jiménez-Barbero, *ChemBioChem* **2008**, *9*, 240.
- [32] Y. J. Shin, R. T. Shafraneck, J. H. Tsui, J. Walcott, A. Nelson, D.-H. Kim, *Acta Biomater.* **2021**, *119*, 75.

- [33] T. Gao, G. J. Gillispie, J. S. Copus, A. K. Pr. Y.-J. Seol, A. Atala, J. J. Yoo, S. J. Lee, *Biofabrication* **2018**, *10*, 034106.
- [34] Z. Dai, J. Ronholm, Y. Tian, B. Sethi, X. Cao, *J. Tissue Eng.* **2016**, *7*, 204173141664881.
- [35] ISO 10993-5:2009 Biological Evaluation of Medical Devices. Part 5: Tests for In Vitro Cytotoxicity. International Organization for Standardization; Geneva, Switzerland **2009**.
- [36] S. Yamada, K. Sugahara, *Curr. Drug Discovery Technol.* **2008**, *5*, 289.
- [37] K. Markstedt, A. Mantas, I. Tournier, H. Martínez Ávila, D. Hägg, P. Gatenholm, *Biomacromolecules* **2015**, *16*, 1489.
- [38] L. Ouyang, R. Yao, Y. Zhao, W. Sun, *Biofabrication* **2016**, *8*, 035020.
- [39] Z. M. Jessop, A. Al-Sabah, N. Gao, S. Kyle, B. Thomas, N. Badieli, W. Hawkins, I. S. Whitaker, *Biofabrication* **2019**, *11*, 045006.
- [40] A. Dank, I. H. A. Aartman, D. Wismeijer, A. Tahmaseb, *Int. J. Implant Dent.* **2019**, *5*, 12.
- [41] Z. Schwartz, J. Y. Martin, D. D. Dean, J. Simpson, D. L. Cochran, B. D. Boyan, *J. Biomed. Mater. Res.* **1996**, *30*, 145.
- [42] X. Cun, L. Hosta-Rigau, *Nanomaterials* **2020**, *10*, 2070.
- [43] S.-M. Lien, L.-Y. Ko, T.-J. Huang, *Acta Biomater.* **2009**, *5*, 670.
- [44] H. Park, X. Guo, J. S. Temenoff, Y. Tabata, A. I. Caplan, F. K. Kasper, A. G. Mikos, *Biomacromolecules* **2009**, *10*, 541.
- [45] M. Mahinroosta, Z. Jomeh Farsangi, A. Allahverdi, Z. Shakoobi, *Mater. Today Chem.* **2018**, *8*, 42.
- [46] Y. Guo, T. Yuan, Z. Xiao, P. Tang, Y. Xiao, Y. Fan, X. Zhang, *J. Mater. Sci.: Mater. Med.* **2012**, *23*, 2267.
- [47] Z. Wu, X. Su, Y. Xu, B. Kong, W. Sun, S. Mi, *Sci. Rep.* **2016**, *6*, 24474.
- [48] D. Eglin, D. Mortisen, M. Alini, *Soft Matter* **2009**, *5*, 938.
- [49] V. Guarino, T. Caputo, R. Altobelli, L. Ambrosio, *AIMS Mater. Sci.* **2015**, *2*, 497.
- [50] E. Alsberg, H. J. Kong, Y. Hirano, M. K. Smith, A. Albeiruti, D. J. Mooney, *J. Dent. Res.* **2003**, *82*, 903.
- [51] M. Criado, J. M. Rey, C. Mijangos, R. Hernández, *RSC Adv.* **2016**, *6*, 105821.
- [52] J. Thiele, Y. Ma, S. M. C. Bruekers, S. Ma, W. T. S. Huck, *Adv. Mater.* **2014**, *26*, 125.
- [53] M. L. Hall, D. A. Krawczak, N. K. Simha, J. L. Lewis, *Osteoarthr. Cartil.* **2009**, *17*, 655.
- [54] Y. P. Singh, A. Bandyopadhyay, B. B. Mandal, *ACS Appl. Mater. Interfaces* **2019**, *11*, 33684.
- [55] F. Mirahmadi, M. Tafazzoli-Shadpour, M. A. Shokrgozar, S. Bonakdar, *Mater. Sci. Eng., C* **2013**, *33*, 4786.
- [56] P. K. Gupta, A. K. Das, A. Chullikana, A. S. Majumdar, *Stem Cell Res. Ther.* **2012**, *3*, 25.
- [57] K. Peltari, E. Steck, W. Richter, *Injury* **2008**, *39*, 58.
- [58] C. Antich, J. De Vicente, G. Jiménez, C. Chocarro, E. Carrillo, E. Montañez, P. Gálvez-Martín, J. A. Marchal, *Acta Biomater.* **2020**, *106*, 114.
- [59] L. D. Solorio, A. S. Fu, R. Hernández-Irizarry, E. Alsberg, *J. Biomed. Mater. Res., Part A* **2010**, *92A*, 1139.
- [60] J. M. Trowbridge, R. L. Gallo, *Glycobiology* **2002**, *12*, 117R.
- [61] A. Cañibano-Hernández, L. Saenz Del Burgo, A. Espona-Noguera, G. Orive, R. M. Hernández, J. Ciriza, J. L. Pedraz, *Mol. Pharmaceutics* **2017**, *14*, 2390.
- [62] K. Motokawa, S. K. Hahn, T. Nakamura, H. Miyamoto, T. Shimoboji, *J. Biomed. Mater. Res., Part A* **2006**, *78A*, 459.
- [63] Y.-L. Chen, H.-C. Chen, H.-Y. Chan, C.-K. Chuang, Y.-H. Chang, Y.-C. Hu, *Biotechnol. Bioeng.* **2008**, *101*, 821.
- [64] J. Hauptstein, T. Böck, M. Bartolf-Kopp, L. Forster, P. Stahlhut, A. Nadernezhad, G. Blahetek, A. Zernecke-Madsen, R. Detsch, T. Jüngst, J. Groll, J. Teßmar, T. Blunk, *Adv. Healthcare Mater.* **2020**, *9*, 2000737.
- [65] S. Ishikawa, K. Iijima, K. Sasaki, M. Hashizume, M. Kawabe, H. Otsuka, *Appl. Sci.* **2018**, *8*, 1398.
- [66] C. L. Deal, R. W. Moskowitz, *Rheum. Dis. Clin. N. Am.* **1999**, *25*, 379.
- [67] R. A. A. Muzzarelli, F. Greco, A. Busilacchi, V. Sollazzo, A. Gigante, *Carbohydr. Polym.* **2012**, *89*, 723.
- [68] W. S. Toh, X.-M. Guo, A. B. Choo, K. Lu, E. H. Lee, T. Cao, *J. Cell. Mol. Med.* **2009**, *13*, 3570.
- [69] Council of Europe. Sterility. *The European Pharmacopoeia*, 9th ed., EDQM, Strasbourg, France **2017**, Ch. 2.6.1.
- [70] A. Zabala, L. Blunt, R. Tejero, I. Llavori, A. Aginagalde, W. Tato, *Surf. Topogr.: Metrol. Prop.* **2020**, *8*, 015002.
- [71] ISO 25178-2 2012 Geometrical product specifications (GPS)—Surface texture: Areal: II. Terms, definitions and surface texture parameters, **2012**.